THE JOURNAL OF BIOLOGICAL CHEMISTRY VOL. 284, NO. 38, pp. 25889–25899, September 18, 2009

Cooperative Regulation of the Interferon Regulatory Factor-1 Tumor Suppressor Protein by Core Components of the Molecular Chaperone Machinery*

Received for publication, May 11, 2009, and in revised form, June 3, 2009 Published, JBC Papers in Press, June 5, 2009, DOI 10.1074/jbc.M109.019505

Vikram Narayan[‡], **Mirjam Eckert**[‡1], **Alicja Zylicz**[§], **Maciej Zylicz**[§], **and Kathryn L. Ball**[‡2]

From the [‡]*Cancer Research UK Interferon and Cell Signalling Group, Cell Signalling Unit, Institute of Genetics and Molecular Medicine, University of Edinburgh, Edinburgh EH4 2XR, Scotland, United Kingdom and the* [§]*International Institute of Molecular and Cell Biology, 02-109 Warsaw, Poland*

Our understanding of the post-translational processes involved in regulating the interferon regulatory factor-1 (IRF-1) tumor suppressor protein is limited. The introduction of mutations within the C-terminal Mf1 domain (amino acids 301–325) impacts on IRF-1-mediated gene repression and growth suppression as well as the rate of IRF-1 degradation. However, nothing is known about the proteins that interact with this region to modulate IRF-1 function. A biochemical screen for Mf1-interacting proteins has identified an L*XX*LL motif that is required for binding of Hsp70 family members and cooperation with Hsp90 to regulate IRF-1 turnover and activity. These conclusions are supported by the finding that Hsp90 inhibitors suppress IRF-1-dependent transcription shortly after treatment, although at later time points inhibition of Hsp90 leads to an Hsp70-dependent depletion of nuclear IRF-1. Conversely, the half-life of IRF-1 is increased by Hsp90 in an ATPase-dependent manner leading to the accumulation of nuclear but not cytoplasmic IRF-1. This study begins to elucidate the role of the Mf1 domain of IRF-1 in orchestrating the recruitment of regulatory factors that can impact on both its turnover and transcriptional activity.

Interferon regulatory factor-1 (IRF-1),[3] the founding member of the interferon regulatory factor family, is a transcription factor that regulates a diverse range of target genes during the response to stimuli such as pathogen infection (1), DNA damage (2, 3), and hypoxia (4). In addition, the loss of *IRF-1* can cooperate with c-Ha-*ras* (5) in cellular transformation; it becomes up-regulated in cells that bear oncogenic lesions (6), and deletions of *IRF-1* are associated with the development of gastric and esophageal tumors, as well as some leukemias (7–9). On the basis of these observations IRF-1 has been characterized as a tumor suppressor protein. Although initially identified as a component of the *IFNβ*-enhanceosome complex, IRF-1 has since been demonstrated to regulate the expression of a large cohort of interferon-responsive genes involved in negative growth control (10–12).

Structurally, IRF-1 includes several domains; prominent among these is a highly conserved N-terminal sequence-specific DNA-binding domain, a transactivation domain, and a C-terminal regulatory domain known as the enhancer (13). The enhancer was originally identified as a region required for maximal IRF-1-mediated transactivation, although it does not have intrinsic transactivation potential (13). More recent structure-function analysis has shown that the enhancer is involved in the recruitment of coactivators to IRF-1 target promoters (14) and that it can facilitate IRF-1-mediated growth suppression (15), as well as being an important determinant of the rate at which IRF-1 is degraded (15–17). Housed within the enhancer is a multifunctional subdomain that we have named Mf1 (Multifunctional 1; amino acids 301–325). This domain impacts on IRF-1-mediated transrepression of the *CDK2* gene (14) and is required for maximal IRF-1-mediated growth suppression (14). Most recently studies have shown that Mf1 is also involved in processing of polyubiquitinated IRF-1 by the proteasome (17). Although the Mf1 is involved in multiple regulatory processes (15, 17), nothing is currently known about the mechanism of action of this region and how, for example, cellular factors interact with the Mf1 domain to modulate IRF-1-dependent gene expression and growth repressor activity or to promote IRF-1 turnover.

In this study, we provide evidence linking IRF-1 to the Hsp70 family and Hsp90, the core components of the molecular chaperone machinery. Originally defined by their role in *de novo* protein folding and the response to cellular stress (18, 19), it is now recognized that the molecular chaperones have diverse functions in processes that include the following: protein folding (19), preventing the aggregation of denatured proteins (20), maintenance of cell signaling and trafficking pathways (21, 22), and the assembly and/or disassembly of multiprotein complexes (23, 24). In addition, Hsp70 and Hsp90 are involved in the regulation of diverse "client" proteins where changes in conformation and activity of mature proteins are the primary goal. Client proteins interact with Hsp70 and/or Hsp90 in a cyclic manner with binding and dissociation being linked to changes in chaperone conformation and the hydrolysis of ATP

* This work was supported by Programme Grant C377/A6355 (to K. L. B.) from Cancer Research UK and a grant from the Polish Ministry of Science and Higher Education (to A. Z. and M. Z.).

[1] Present address: Dept. of Biochemistry, University of Lausanne, Chemin des Boveresses 155, CH-1066 Epalinges, Switzerland.

[2] To whom correspondence should be addressed: Cell Signalling Unit, University of Edinburgh Cancer Research Centre, Crewe Road South, Edinburgh EH4 2XR, Scotland, UK. Tel.: 44-131-777-3560; E-mail: kathryn.ball@ed.ac.uk.

[3] The abbreviations used are: IRF-1, interferon regulatory factor-1; ELISA, enzyme-linked immunosorbent assay; GAPDH, glyceraldehyde-3-phosphate dehydrogenase; mAb, monoclonal antibody; GST, glutathione *S*-transferase; RT, reverse transcription; WT, wild type.

(25, 26). Here a requirement for the C-terminal Mf1 domain of IRF-1 in the recruitment of Hsp70 proteins is demonstrated. In turn it is shown that Hsp70 recruits Hsp90 and together they have an impact on the turnover, localization, and activity of IRF-1. The data highlight a novel IRF-1 interaction that contributes to its activation pathway suggesting that the molecular chaperones are key components of a regulatory network that maintains IRF-1 tumor suppressor function.

MATERIALS AND METHODS

Chemicals, Antibodies, and Peptides—Antibodies were used at 1 μg/ml and were anti-IRF-1 and anti-GFP (BD Biosciences), anti-GAPDH (Abcam), anti-FLAG and anti-GST (Sigma), anti-Chk1 (G-4), anti-caspase-3 (Santa Cruz Biotechnology), and anti-Hp1α (Upstate). All antibodies to heat shock proteins were from StressGen. Secondary antibodies were purchased from Dako Cytomation. 17AAG and radicicol (AG Scientific) were dissolved in DMSO to 1 mg/ml and used as detailed in the figure legends. MG-132 (Calbiochem) was dissolved in DMSO to 10 mM and used as indicated. Cycloheximide (Supelco) was dissolved in water to 5 mg/ml and used at 30 μg/ml. Peptides were from Chiron Mimotopes and were synthesized with a biotin tag at the N terminus with an SGSG spacer.

Cell Culture and Transfection—A375 and H1299 cells were cultured in Dulbecco's modified Eagle's medium and RPMI 1640 medium (Invitrogen), respectively, supplemented with 10% (v/v) fetal bovine serum (Autogen Bioclear) and 1% (v/v) penicillin/streptomycin mixture (Invitrogen). Cells were seeded 24 h before transfection. DNA (250 ng unless stated otherwise) was transfected into the cells using Attractene (Qiagen) as described in the manufacturer's instructions.

Cell Lysis and Immunoblotting—Cells were lysed in Triton Lysis Buffer (50 mM Hepes, pH 7.5, 0.1% (v/v) Triton X-100, 150 mM NaCl, 10 mM NaF, 2 mM dithiothreitol, 0.1 mM EDTA, 20 μg/ml leupeptin, 1 μg/ml aprotinin, 2 μg/ml pepstatin, 1 mM benzamidine, 10 μg/ml soybean trypsin inhibitor, 2 mM Pefabloc, 1.6 mM EGTA) unless otherwise indicated. 2× volume lysis buffer was added to the cell pellet and incubated on ice for 20 min, followed by centrifugation at 16,000 × *g* for 15 min at 4 °C. Supernatant was collected and the protein quantified by Bradford assay. Samples were analyzed by SDS-PAGE and transferred to nitrocellulose (Protran, Schleicher & Schuell). The membranes were blocked using 5% (w/v) nonfat milk powder in phosphate-buffered saline + 0.1% (v/v) Tween 20 (PBST) for 1 h at room temperature. Membranes were then incubated with primary antibody at 1 μg/ml for 1 h at room temperature (or overnight at 4 °C) followed by the secondary antibody (1:2000) for 1 h. The immunoblots were washed extensively between each step with PBST. Antibody binding was detected by enhanced chemiluminescence.

Peptide Affinity Chromatography and Protein Identification—A375 cell lysate (as above) was treated with avidin (Sigma) at 40 μg/ml for 30 min on ice and centrifuged at 16,000 × *g* for 5 min. Treated lysates were pre-cleared using Sepharose-4B (Sigma) beads for 1 h at 4 °C and applied to a peptide column. Peptide affinity columns were prepared using Mobicol column jackets (MoBiTec) containing 50 μl of streptavidin-agarose with biotin peptide. Enough biotinylated peptide to saturate the streptavidin-agarose bead binding sites was used (Sigma) and incubated with the beads for 1 h at room temperature, and the column was then washed three times with Buffer W (100 mM Tris-HCl, pH 8.0, 150 mM NaCl, 1 mM EDTA, 1 mM benzamidine) to remove unbound peptide. Cleared lysate (0.5 mg) was added to the column and incubated with the resin for 1 h at room temperature. The column was washed four times with phosphate-buffered saline + 0.2% Triton X-100 and one time with Buffer W. Bound proteins were eluted by boiling in SDS sample buffer. Eluates were run on a 4–12% NuPAGE gel (Invitrogen), and stained with colloidal blue (Invitrogen). Bands were excised and trypsinized in the gel prior to analysis by one-dimensional nanoliquid chromatography-tandem mass spectrometry using a 4000 QTrap (Applied Biosystems) tandem mass spectrometry system (Fingerprints Proteomics Facility, University of Dundee). The raw QTrap data were analyzed using Mascot. Alternatively, SDS-PAGE-separated samples were transferred onto nitrocellulose and immunoblotted as required.

Immunoprecipitation and ELISA—OneSTREP (IBA)-tagged IRF-1 (or empty vector) was transfected into A375 cells as described above. Post-transfection (24 h), cells were harvested and lysed in Triton Lysis Buffer. Following this, tagged complexes were purified according to the manufacturer's instructions and analyzed by SDS-PAGE/immunoblot. For the ELISA, purified recombinant Hsp70 or Hsc70 (250 ng) was coated onto a white 96-well plate (Fisher) in 0.1 M $NaHCO_3$ buffer, pH 8.6, at 4 °C. Nonreactive sites were blocked using phosphate-buffered saline containing 3% bovine serum albumin. Empirically determined amounts of the protein of interest (GST, GST-IRF-1 WT, or GST-IRF-1 ΔEnh) were added in 1× Reaction Buffer (25 mM Hepes, pH 7.5, 50 mM KCl, 10 mM $MgCl_2$, 5% (v/v) glycerol, 0.1% (v/v) Tween 20, 2 mg/ml bovine serum albumin) for 1 h at room temperature. After washing extensively in phosphate-buffered saline containing 0.1% (v/v) Tween 20, binding was detected using anti-GST and horseradish peroxidase-tagged anti-mouse antibodies, and electrochemical luminescence was quantified using a luminometer (Labsystems; Fluoroskan Ascent FL).

Size Exclusion Chromatography—A375 cells were lysed in fast protein liquid chromatography Lysis Buffer (20 mM Hepes, pH 7.5, 0.25 M NaCl, 10% (w/v) sucrose, 10% (v/v) glycerol, 0.1% (v/v) Triton X-100, 5 mM NaF, 2 mM β-glycerophosphate, 1 mM dithiothreitol, 20 μg/ml leupeptin, 1 μg/ml aprotinin, 2 μg/ml pepstatin, 1 mM benzamidine, 10 μg/ml soybean trypsin inhibitor, 2 mM Pefabloc, 1.6 mM EGTA) and passed through a 0.45-μm filter. Lysate generated from 1 × 10-cm plate extracted in 500 μl of buffer was loaded onto a 25-ml Superose-6 column (Amersham Biosciences) equilibrated in fast protein liquid chromatography column buffer (20 mM Hepes, pH 7.5, 0.25 M NaCl, 5% (w/v) sucrose, 5% (v/v) glycerol, 0.05% (v/v) Triton X-100, 5 mM NaF, 1 mM dithiothreitol, 1 mM benzamidine). The flow rate was adjusted to 0.4 ml/min, and 0.5-ml fractions were collected. Fractions were precipitated using trichloroacetic acid and analyzed by SDS-PAGE/immunoblot.

mRNA Extraction and RT-PCR—H1299 cells were treated with 17AAG as indicated and harvested. Half of the cells were lysed in Triton Lysis Buffer, and analyzed for protein. From the remaining 50% of cells, RNA was extracted using the RNeasy

mini kit (Qiagen). The extracted RNA was reverse-transcribed using the Omniscript RT kit (Qiagen). PCR was performed using PCR Master Mix (VH Bio) and an annealing temperature of 55 °C for 25 cycles. Primer sequences were as follows: IRF-1, TTAATAAAGAGGAGATGATCTTCC/CCTGCTTTGTATCGGCCTGTGTGA and GAPDH, GTCAGTGGTGGACCTGACCT/ACCTGGTGCTCAGTGTAGCC.

Luciferase Assay—For luciferase reporter assays, cells were cultured in 24-well plates and transfected with pCMV-Renilla/Luc (60 ng) together with either TLR3-Firefly/Luc WT or mutant (−ISRE; 140 ng). Luciferase assays were performed 24 h post-transfection using the Dual Luciferase® reporter assay system (Promega) according to the manufacturer's instructions. Luminescence was quantified using a Fluoroskan Ascent F1 luminometer (Labsystems). Signals were normalized using the internal control (*Renilla* luciferase signal). Results are represented as mean ± S.D.

Subcellular Fractionation and Half-life Analysis—Subcellular fractionation was carried out using the ProteoExtract kit (Calbiochem) according to the manufacturer's instructions. For the half-life determination, A375 cells in 35-mm plates were transfected as indicated in the figure legends. Post-transfection (24 h), the cells were treated with 30 μg/ml cycloheximide and harvested at the indicated time points. Samples were fractionated as described above. Nuclear fractions (40 μg) were analyzed by SDS-PAGE/immunoblot. Band intensity was quantified using Scion Imaging software. The intensity of the zero time point was taken as 100%, and the others were measured relative to this. A graph of ln(% protein remaining) against time was plotted to obtain a linear graph. The equation of the graph was used to calculate the x axis value corresponding to y = ln(50%). This value represents the calculated half-life.

RESULTS

Identification of the Molecular Chaperone Hsp70 as a Novel IRF-1-binding Protein—The C-terminal enhancer region of IRF-1 (Fig. 1*A*) is an important regulatory domain (14–16). Of particular interest is the Mf1 region (amino acids 301–325) that is essential for maximal IRF-1-mediated growth suppression (15) and that plays a key role in determining the rate of IRF-1 degradation (17). In a quest to identify factors that mediate the regulatory functions of the Mf1 domain, we adapted a biochemical screen (Fig. 1*B*) developed to identify protein interaction motifs in IRF-1.[4] A biotin-labeled peptide (pep-(301–320)) based on amino acids 301–320 of IRF-1 was immobilized using streptavidin-agarose and used to generate an affinity column (50-μl volume). The column was loaded with A375 cell extract and washed extensively prior to the recovery of bound proteins. Eluted protein was analyzed using SDS-PAGE on 4–12% gradient gels and individual bands identified by mass fingerprinting (Fig. 1*C, left panel*). The major protein band pulled out by the pep-(301–320) column (Fig. 1*C, left panel arrow*) was analyzed by mass fingerprinting and was found to contain both constitutive and inducible members of the Hsp70 family of molecular chaperones. Immunoblot analysis using an Hsp70-specific antibody was used to confirm the mass fingerprint identification (Fig. 1*C, right panel*).

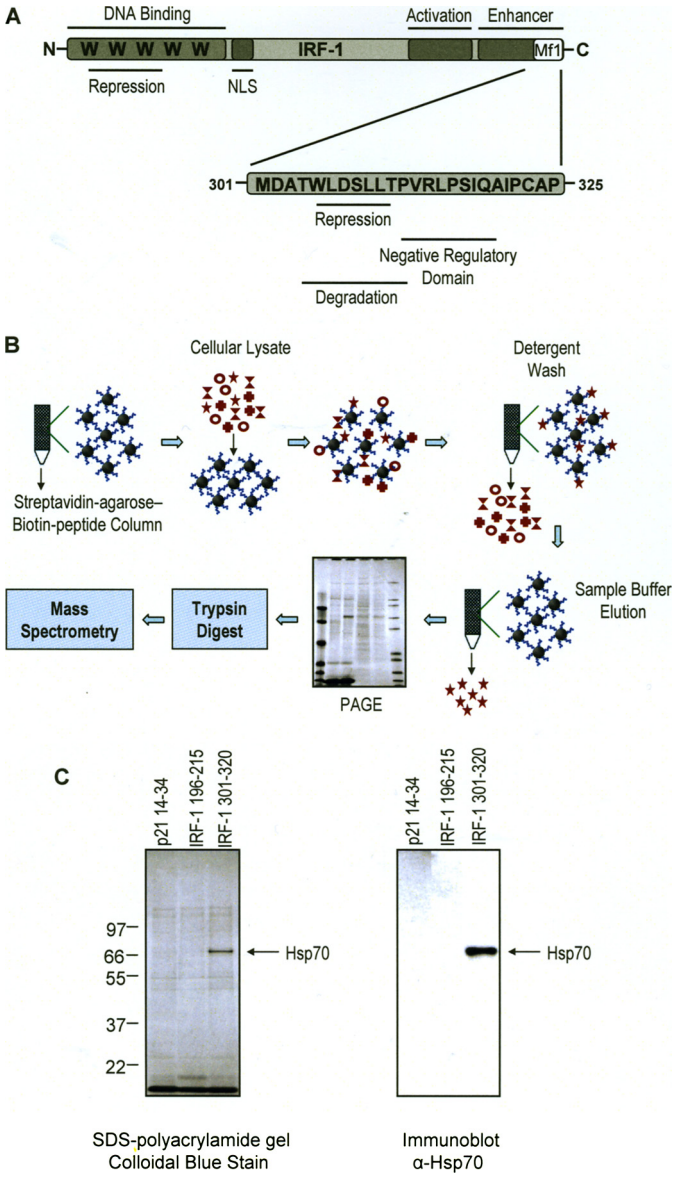

FIGURE 1. **Identification of the molecular chaperone Hsp70 as an IRF-1-interacting protein.** *A*, IRF-1 domain organization. *NLS*, nuclear localization signal; *Mf1*, multifunctional domain 1. *B*, overview of the method used to identify the C-terminal IRF-1-interacting proteins. *C*, eluates from the method depicted in *B* were run on 4–12% gradient gels and stained with colloidal blue (*left panel*). *Right panel*, duplicate gel was run and transferred to nitrocellulose. The immunoblot was developed using the Hsp70 mAb (clone SPA-810). In addition to IRF-1 peptide 301–320, a p21 peptide (amino acids 15–34) and a second IRF-1 peptide (amino acids 196–215) were used as controls to check for nonspecific binding.

Hsp70 Binds Directly to IRF-1—The data presented above suggest that Hsp70 family members can bind to a 20-amino acid peptide based on part of the Mf1 domain. Based on this observation, evidence was sought that Hsp70 could bind the Mf1 region of IRF-1 when found in the context of the full-length protein. First, size exclusion chromatography was used to determine whether cellular IRF-1 and Hsp70 coeluted in a manner consistent with complex formation in the cellular environment. Using a Superose-6 column, IRF-1 from A375 cell lysate was found to elute in three distinct peaks (Fig. 2*A*) as follows:

[4] V. Narayan and K. L. Ball, unpublished data.

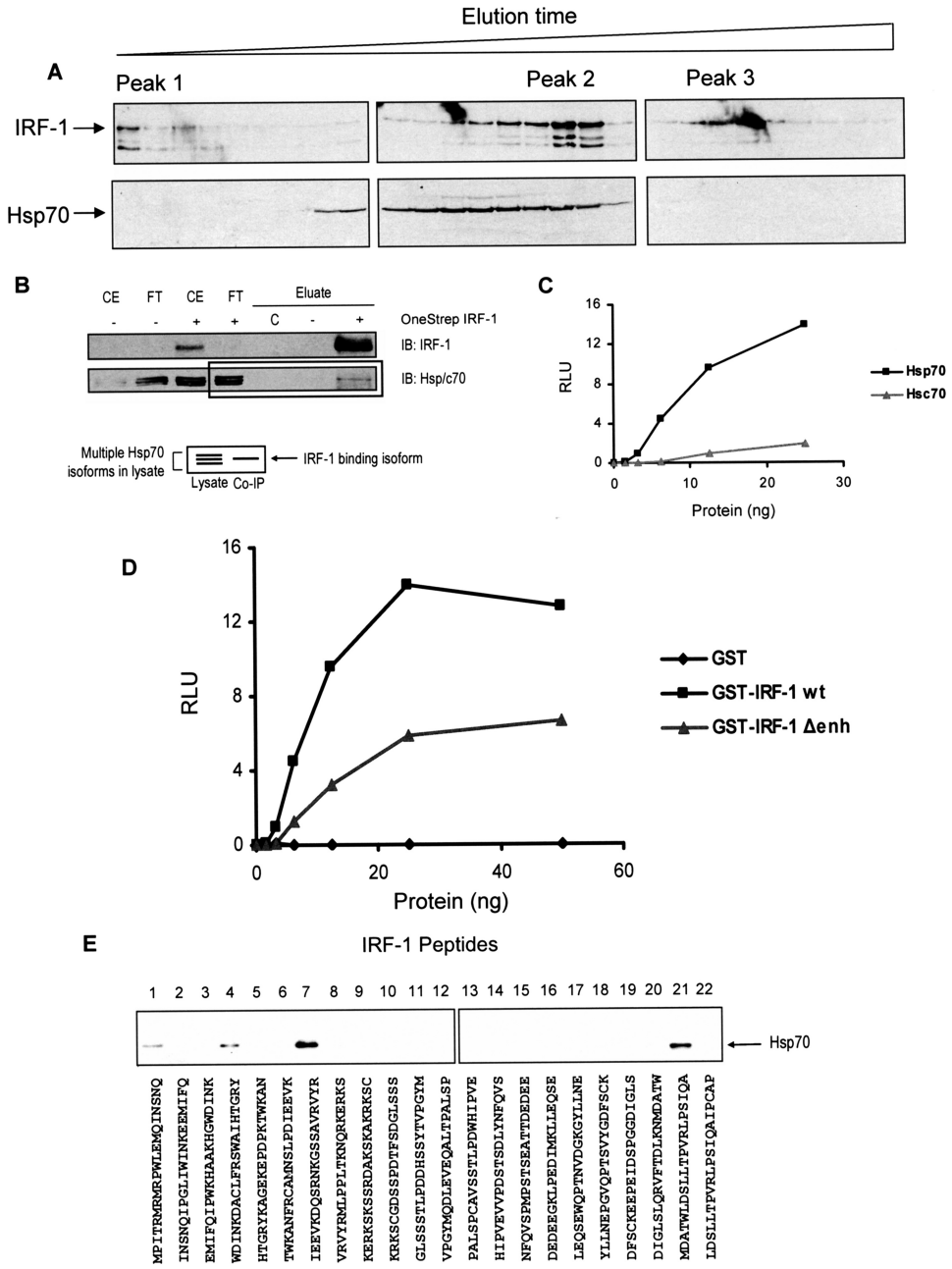

FIGURE 2. **Hsp70 interacts with IRF-1 *in vitro* and in cells.** *A,* lysate from A375 cells stably expressing IRF-1 was analyzed by size exclusion chromatography. Protein from each fraction (0.5 ml) was precipitated using trichloroacetic acid and analyzed by 12% SDS-PAGE/immunoblot developed using IRF-1 mAb and anti-Hsp/c70. *B,* immunoblot (*IB*) of OneStrep-IRF-1 isolated using Streptactin from A375 cells that had been transiently transfected with OneStrep-IRF-1 or empty vector as indicated. The immunoblots were probed for IRF-1 and Hsp/c70 (SPA-822). Crude cell extract (*CE*) and flow-through (*FT*) from the Streptactin column are shown, and *C* is a bead only control. Inserted is a schematic of the gel showing that although there are three Hsp/c70 isoforms picked up by the antibody, only one of these comes down with IRF-1. *Co-IP*, coimmunoprecipitation. *C,* recombinant Hsp70 and Hsc70 purified from *E. coli* (50 ng) were coated onto a microtiter plate and incubated with a titration (0–25 ng) of GST-IRF-1. Binding was detected using an anti-GST antibody and enhanced chemiluminescence. Protein concentration against binding, expressed as relative light units (*RLU*), is shown. The results are representative of three separate experiments. *D,* as in *C*, Hsp70 was coated onto an ELISA plate and incubated with a titration (0–50 ng) of GST, GST-IRF-1 WT, or GST-IRF-1Δenh. Protein concentration against binding, expressed as relative light units (*RLU*), is shown. The results are representative of four separate experiments. *E,* panel of overlapping IRF-1 peptides spanning the entire length of the protein was used to generate affinity columns (see Fig. 1*B*) to determine whether Hsp70 from A375 lysate bound to sites on IRF-1 other than the Mf1 domain. Bound proteins, including Hsp70, were eluted in sample buffer and analyzed by SDS-PAGE/immunoblot using anti-Hsp70 mAb (SPA-810). The results are representative of two independent experiments.

one in the void volume (peak 1) and two that were included (peaks 2 and 3), indicative of multiple IRF-1-containing complexes. Peak 2 coeluted with fractions that also contained Hsp70 suggesting that cellular IRF-1 and Hsp70 may be present in the same complex. To provide further evidence of Hsp70-IRF-1 complex formation in cells, OneStrep-tagged IRF-1 was expressed in A375 cells and captured using a Streptactin column. Fig. 2*B* shows that OneStrep-IRF-1 was quantitatively depleted from cell extracts by Streptactin with no tagged-IRF-1 detectable in the flow-through. When OneStrep-IRF-1 bound protein was analyzed for the presence of 70-kDa heat shock protein family members using an antibody to Hsp/c70, of the three isoforms detected in the cell extract, only one isoform bound specifically to IRF-1 (Fig. 2*B*), and no binding was detected in the control lane. This suggests that the interaction between full-length IRF-1 and the cellular Hsp70 proteins is fairly specific as one isoform bound with a higher affinity.

The above experiments suggest that Hsp70 family members can form a complex with IRF-1 in cells and that the interaction is specific to certain Hsp70 isoforms; however, they do not address whether the interaction is direct or if additional cellular factors are required. To determine whether Hsp70 could bind directly to IRF-1, we used recombinant proteins purified from *E. coli*. Hsp70 and Hsc70 (27) bound to GST-IRF-1 when they were immobilized (Fig. 2*C*). However, the affinity of Hsp70 was an order of magnitude greater than that of Hsc70 suggesting that IRF-1 interacts preferentially with Hsp70.

As the interaction between IRF-1 and Hsp70 was identified using an Mf1 domain peptide (pep-(301–320); Fig. 1*C*), we determined whether the C-terminal domain was required for Hsp70 to bind full-length IRF-1. To do this a C-terminal IRF-1 deletion mutant (IRF-1ΔEnh (15) was purified from an *E. coli* expression system. A comparison of Hsp70 binding to purified WT and ΔEnh IRF-1 (Fig. 2*D*) suggests that deletion of the C-terminal Mf1 domain leads to a significant decrease in the affinity of IRF-1 for Hsp70 supporting a role for the enhancer domain in engaging the chaperone

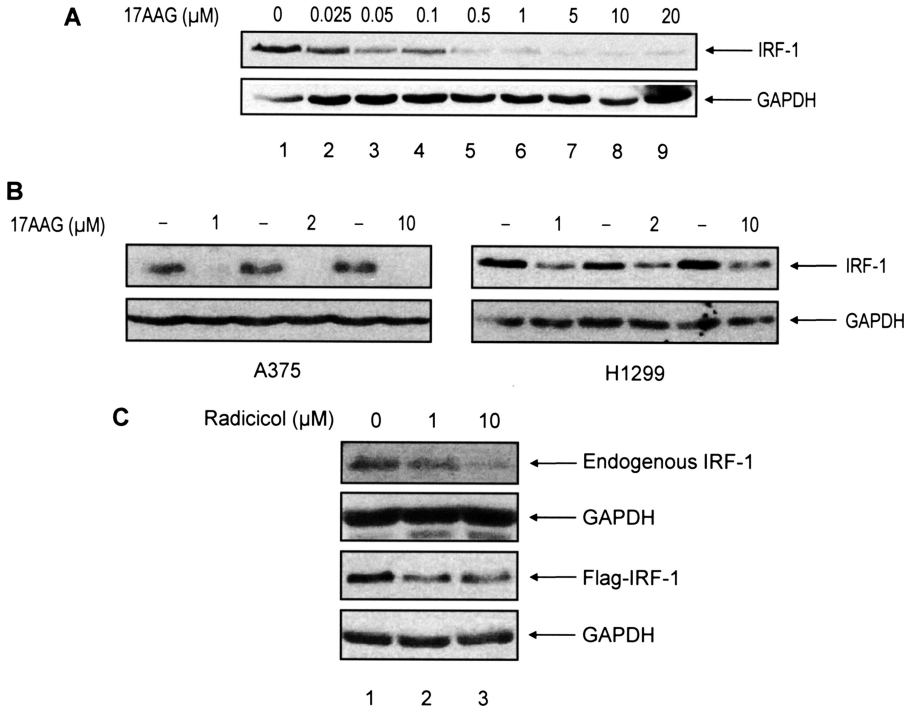

FIGURE 3. **Hsp90 inhibition induces a decrease in IRF-1 protein levels.** *A*, A375 cells were treated with the indicated concentrations of 17AAG for 12 h. Cells were lysed and analyzed by SDS-PAGE/immunoblot developed using IRF-1 mAb and anti-GAPDH. The experiment is representative of at least two individual experiments. *B*, A375 and H1299 cells were treated with 17AAG or the DMSO carrier as indicated for 20 h. Lysates were analyzed as above and are representative of two separate experiments. *C*, A375 cells (untransfected or transfected with FLAG-IRF-1) were treated with the indicated concentrations of radicicol for 20 h. Lysates were analyzed by SDS-PAGE/immunoblot, and probed for IRF-1 and GAPDH as above.

machinery. In addition, as residual Hsp70 binding to the ΔEnh IRF-1 protein was detected, the interaction between IRF-1 and Hsp70 is likely to be complex, involving more than one interface. To confirm the presence of an additional interface(s) for Hsp70 in IRF-1, we used a series of overlapping peptides that spanned the length of IRF-1 and asked if any of these peptides could bind to Hsp70 from cell lysates. Fig. 2*E* shows that Hsp70 bound predominantly to the Mf1 domain and to a second peptide based on a region from the N-terminal DNA binding domain of IRF-1 (amino acids 91–110). As the crystal structure for the N-terminal domain of IRF-1 has been solved (28), we were able to see that this region of IRF-1 forms a solvent-exposed flexible loop (data not shown). Thus, IRF-1-Hsp70 complex formation appears to require at least two distinct interfaces, one of which is composed of a solvent-exposed flexible loop.

Inhibition of Hsp90 Decreases IRF-1 Protein Levels—Hsp70, together with a second molecular chaperone Hsp90, is an essential component of a multiprotein complex that interacts with key regulatory factors involved in the control of cellular proliferation, differentiation, and death. Although Hsp90 has been demonstrated to interact directly with some client proteins *in vitro,* there is speculation that in the cellular environment Hsp90 will inevitably function together with Hsp70 (25, 29). As the results presented above suggested that IRF-1 can interact specifically with Hsp70 both *in vitro* and in a cellular environment, we sought to determine whether IRF-1 was also a client of the Hsp90 chaperone complex. Hsp90 client proteins are targeted for proteasomal degradation upon treatment with Hsp90-specific inhibitors such as 17AAG and radicicol (30, 31). When A375 cells were treated with a titration of 17AAG (25 nM to 20 μM), IRF-1 protein steady state levels decreased by 12 h using concentrations of the drug in the low nanomolar range (Fig. 3*A*, compare *lanes 3* and *4* with *lane 1*). The effect of 17AAG on IRF-1 was verified in a second cell line as IRF-1 steady state levels were reduced by the drug in H1299 cells, as well as in A375 cells (Fig. 3*B*).

To confirm that the 17AAG-induced decrease in the steady state levels of the IRF-1 protein was because of Hsp90 inhibition, and not an off-target effect of the drug itself, a second Hsp90 inhibitor, radicicol, was used. Although the mechanism of action of radicicol and 17AAG are similar (both bind to and block the ATP-binding site on Hsp90), radicicol is structurally unrelated to 17AAG. Fig. 3*C* (compare *lanes 2* and *3* to *lane 1*) demonstrates that, similar to 17AAG, radicicol treatment causes a decrease in IRF-1 protein levels.

Effect of 17AAG on IRF-1 Is Post-translational—To determine at which stage in the IRF-1 regulatory pathway Hsp90 was operating, we first asked whether 17AAG was able to act on exogenous as well as endogenous IRF-1. Fig. 4*A* shows that IRF-1 proteins expressed in an untagged form (*lanes 3* and *4*) and as a FLAG fusion protein (*lanes 5* and *6*), like endogenous IRF-1 (*lanes 1* and *2*), were sensitive to treatment with 17AAG, suggesting that the drug was not functioning through an effect on the IRF-1 promoter. This conclusion was supported by data showing that 17AAG used at either 1 or 10 μM had no effect on IRF-1 mRNA levels (Fig. 4*B*). As Hsp90 inhibitors have been shown to stimulate degradation of client proteins via the ubiquitin-mediated proteasome pathway, we tested whether 17AAG-dependent IRF-1 loss was sensitive to the proteasome inhibitor MG132. As shown in Fig. 4*C*, the effect of 17AAG on IRF-1 protein levels was partially lost upon treatment with MG132 (compare *lanes 1* and *3* with *lane 4*), suggesting that proteasome-dependent degradation may play a role in the decrease in IRF-1 steady state levels observed upon inhibition of Hsp90 and that the effect of 17AAG is post-translational.

Hsp90 Inhibition Modulates IRF-1 Transcriptional Activity—Treatment of cells with 17AAG led to a decrease in IRF-1 protein levels at 12 h post-treatment; however, at earlier time points the steady state levels of IRF-1 were not affected significantly by Hsp90 inhibition (Fig. 5*A*). The time-dependent nature of 17AAG was exploited to assess its effect on the ability of endogenous IRF-1 to activate transcription at time points where no change in total IRF-1 protein levels was seen. Using a

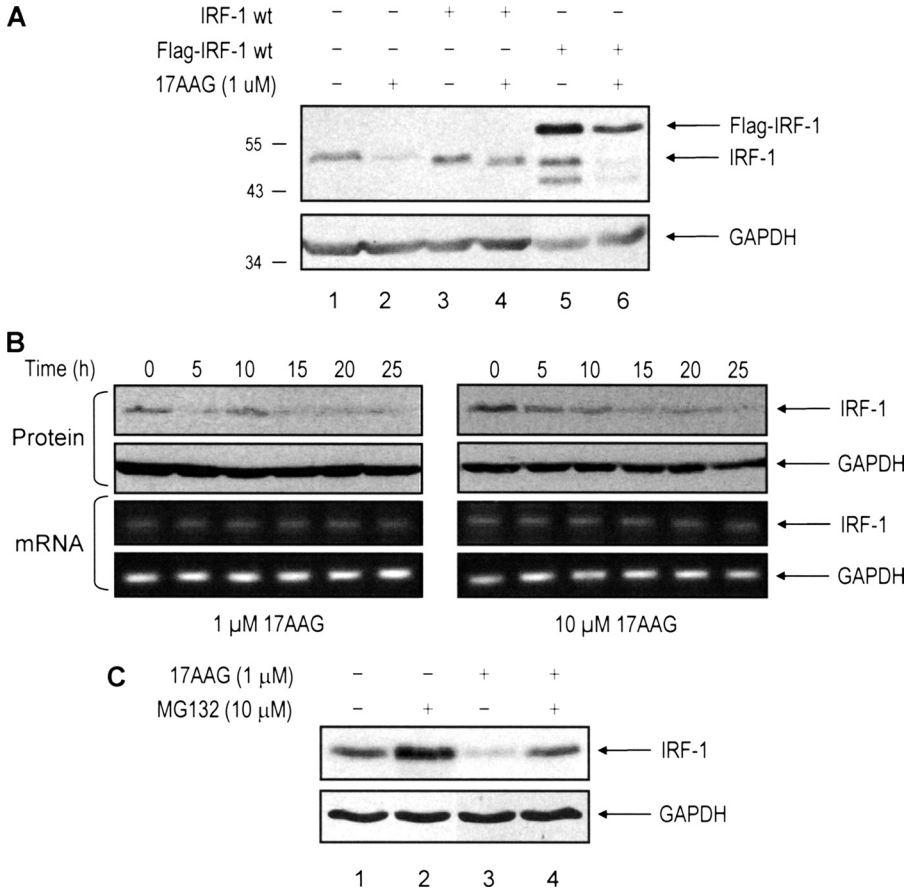

FIGURE 4. **17AAG-dependent loss of IRF-1 is post-translational.** *A*, A375 cells were transiently transfected with pcDNA3-IRF-1 (*IRF-1 wt*), FLAG-IRF-1, or empty vector as indicated and treated with 17AAG (1 μM) 24 h later. Lysates were analyzed by SDS-PAGE/immunoblot developed using IRF-1 mAb and anti-GAPDH. *Lanes 1* and *2* were loaded with 75 μg of total protein so that endogenous IRF-1 could be detected, whereas 25 μg was loaded into the other lanes to detect the transfected protein. The data are representative of at least two separate experiments. *B,* H1299 cells were treated with the indicated concentrations of 17AAG and harvested at various times post-treatment. Half of the cells were used to analyze IRF-1 and GAPDH protein levels by SDS-PAGE/immunoblot, and the remainder of the cells were used to measure IRF-1 and GAPDH mRNA levels by RT-PCR. The data are representative of two experiments. *C,* A375 cells were treated with 17AAG (1 μM) for 12 h prior to the addition of MG132 for a further 4 h. Lysates were analyzed as above and are representative of two separate experiments.

reporter in which the *TLR3* promoter, an IRF-1 target gene (32), was linked to the expression of luciferase, 17AAG (1 μM) treatment consistently caused a decrease in IRF-1 activity prior to decreases in IRF-1 steady state levels (Fig. 5*B*). As IRF-1 is described as a relatively weak transcriptional activator (13), even small changes in its activity are likely to have a significant impact on its biological function. Fig. 5*C* shows that the 17AAG effect was specific for IRF-1 as a TLR3 control plasmid minus the IRF-1 consensus site was not activated in A375 cells.

Inhibition of Hsp90 by 17AAG therefore has a bi-phasic effect on IRF-1; in the early signaling phase, IRF-1 activity as a transcriptional activator is inhibited, and in a second phase, IRF-1 protein levels are down-regulated through a post-translational pathway that can be blocked by proteasome inhibition.

Hsp90 Regulates IRF-1 Turnover and Nuclear Accumulation—The degradation of IRF-1 upon inhibition of Hsp90 suggests that it is an Hsp70/Hsp90 client protein. To determine the normal role of the chaperone system in the pathways leading to regulation of IRF-1, A375 cells were transiently transfected with FLAG-Hsp90. Both the α- and β-isoforms of Hsp90 produced an increase in the amount of endogenous IRF-1 protein detected (Fig. 6*A*). Furthermore, Hsp90-mediated increases in IRF-1 were dependent on its ATPase activity (Fig. 6*B*). Thus, an Hsp90 mutant that could bind to but not hydrolyze ATP (Fig. 6*B, lanes 4–6, E46A*) had no effect on IRF-1 protein levels under conditions where WT Hsp90 increases the levels of IRF-1 (*lanes 1–3*). In addition, a dominant negative form of Hsp90 (Fig. 6*B, lanes 7–9, D93N*), which is incapable of binding ATP, has a similar effect to 17AAG, producing a decrease in IRF-1 protein levels.

IRF-1 is normally distributed between the cytoplasmic and the nuclear compartments of the cell, with a substantial proportion in the nucleus. Cellular fractionation studies were therefore employed to determine whether Hsp90 affected the balance between these two pools. Fig. 6*C* shows that Hsp90 preferentially increases the pool of nuclear IRF-1, with no increase detected in the cytoplasmic fraction (compare *lane 3* with *lane 1*). Conversely, inhibition of Hsp90 by 17AAG caused a preferential loss of protein from the nuclear pool when compared with the cytoplasmic pool (Fig. 6*D*, compare *lanes 3* and *7* with *lanes 1* and *5*). When the half-life of IRF-1 was determined (Fig. 6*E*) in the nuclear fraction of cells overexpressing either Hsp90α or Hsp90β, a decrease in the rate of IRF-1 degradation with the half-life going from 40 min in control cells to ~60 min in the presence of overexpressed Hsp90 was seen (Fig. 6*E, lower panel*).

The results presented in this section support a model where Hsp90 favors the accumulation of nuclear IRF-1 through increases in steady state levels resulting from a decrease in the rate of IRF-1 degradation. However, we cannot exclude the possibility that Hsp90 might also be involved in transport of IRF-1 into the nucleus as has been demonstrated for p53 (33).

Hsp90 Regulation of IRF-1 Is Mediated by Hsp70 Binding—The discovery of Hsp70 as a C-terminal IRF-1-binding protein led us to identify Hsp90 as a key regulator of IRF-1 in the cellular environment. To address whether the regulation of IRF-1 by Hsp90 is mediated through Hsp70, and particularly through binding of Hsp70 to the enhancer domain of IRF-1, we first determined the effect of dominant negative Hsp70 (Fig. 7*A, K71S*, *lanes 5* and *6*) on the ability of 17AAG to modulate IRF-1 steady state levels. Expression of the Hsp70/K71S mutant by itself led to a reduction of IRF-1 steady state levels when com-

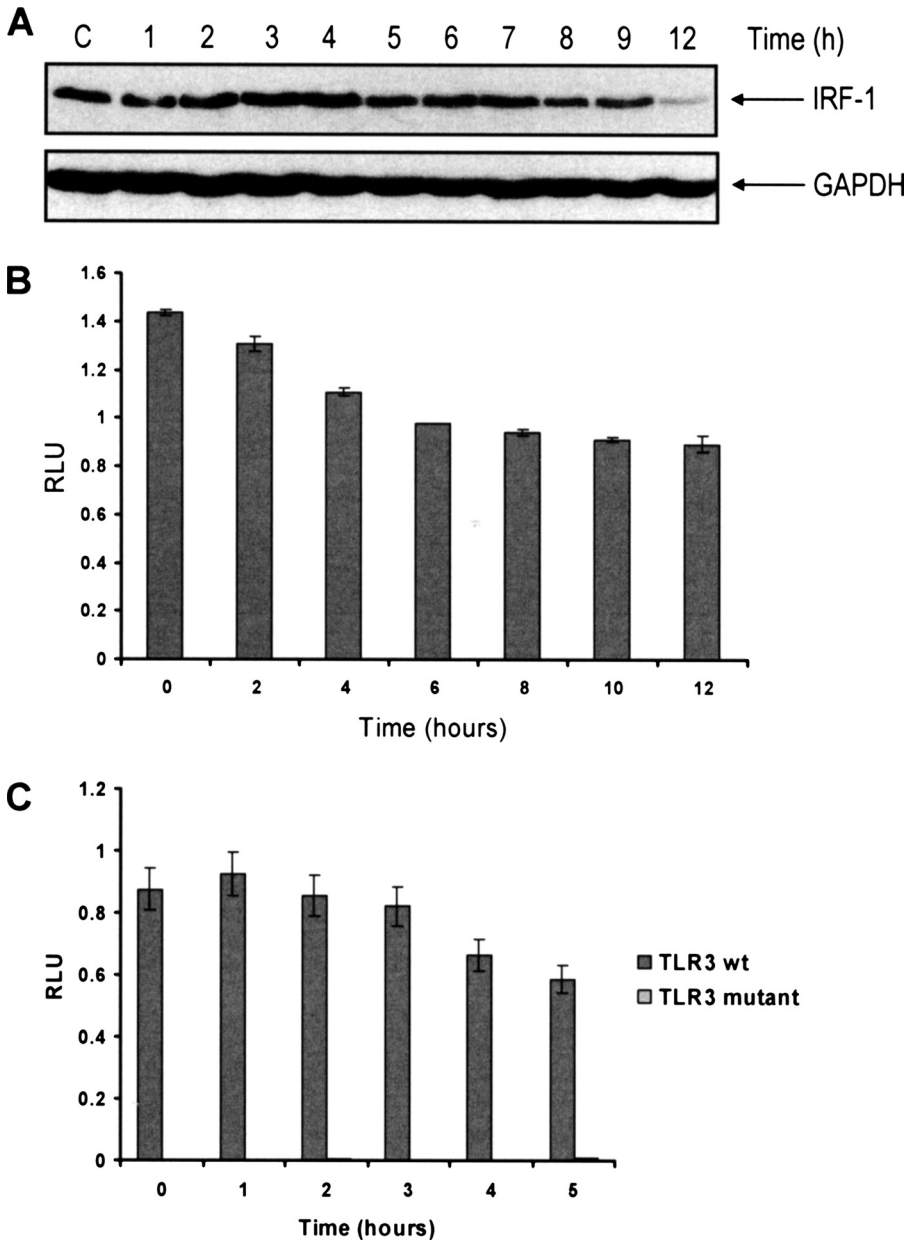

FIGURE 5. **Hsp90 inhibition affects IRF-1 transcriptional activity.** *A,* A375 cells were treated with 17AAG (1 μM) for the indicated times. Lysates were analyzed by SDS-PAGE/immunoblot developed using IRF-1 mAb and anti-GAPDH. *C* is DMSO-treated control cells, and the results are representative of at least three individual experiments. *B,* H1299 cells were cotransfected with a TLR3-fireflyLUC reporter plasmid (140 ng), and control *Renilla*-LUC (60 ng). Post-transfection (24 h), the cells were treated with 17AAG (1 μM) and harvested at the indicated times. Dual luciferase assays were performed, and the results were normalized by expressing TLR3-fireflyLUC/*Renilla* activity in relative light units (*RLU*) as the mean ± S.D. *C,* as above except that a control TLR3 plasmid (TLR3 mutant) lacking the interferon-stimulated response element is included.

pared with control cells and to cells transfected with WT Hsp70 (Fig. 7*A,* compare *lane 5* with *lane 1*). In addition, in the presence of the K71S Hsp70 mutant protein, 17AAG was unable to further reduce the levels of IRF-1 under conditions where levels were significantly decreased in control cells. Next we asked whether the down-regulation of IRF-1 steady state levels in 17AAG-treated cells required its Mf1 domain by using an enhancer domain deletion mutant. Under conditions where 17AAG decreased the expression of both endogenous and transfected WT IRF-1 protein, it had no effect on an IRF-1 mutant protein from which the enhancer domain had been deleted (Fig. 7*B, lanes 5* and *6*). In fact the levels of the IRF-1ΔEnh mutant increased rather than decreased in 17AAG-treated H1299 cells (IRF-1Δenh low exp), suggesting that this protein is resistant to Hsp70-mediated degradation. As a control we determined that the levels of the known Hsp90 clients Chk1 and p53 decrease in response to 17AAG in the same samples where IRF-1Δenh protein was seen to increase (Fig. 7*B,* compare *lanes 5* and *6*).

Fine mapping of the interaction between Hsp70 and the Mf1 domain peptide of IRF-1 was carried out to identify critical contact residues that could then be manipulated to make more specific IRF-1 Hsp70-binding mutants. A library of IRF-1 pep-(301–320) peptides was synthesized in which each amino acid was sequentially replaced with an alanine residue, and the pep-(301–320) library was used to generate a series of affinity columns. Cell lysate was loaded onto the columns, and following extensive washing the columns were eluted, and bound protein was analyzed by immunoblot to identify peptides that showed reduced binding to cellular Hsp70. Using this approach we found that Hsp70 bound to a discrete interaction motif that included a coregulator signature (L*XX*LL) motif and a number of proline residues (Fig. 7*C*). Using the information obtained by fine mapping the Hsp70 interaction with the Mf1 domain of IRF-1, a mutant construct was used where alanine residues had been introduced into the L*XX*LL motif (15). When the effect of radicicol on wild-type and L*XX*LL mutant IRF-1 was compared, the levels of endogenously and exogenously expressed wild-type IRF-1 decreased following radicicol treatment (Fig. 7*D,* compare *lanes 2* and *4* with *1* and *3*) while those of the L*XX*LL mutant protein did not decrease, but similar to ΔEnh IRF-1 (Fig. 7*B*), the amount of protein was increased by Hsp90 inhibition (Fig. 7*D, lanes 5* and *6*). The data presented in this section lend support to the hypothesis that Hsp70 binding to an interaction motif within the Mf1 domain of IRF-1 mediates Hsp90-dependent modulation of IRF-1 steady state levels in the nucleus.

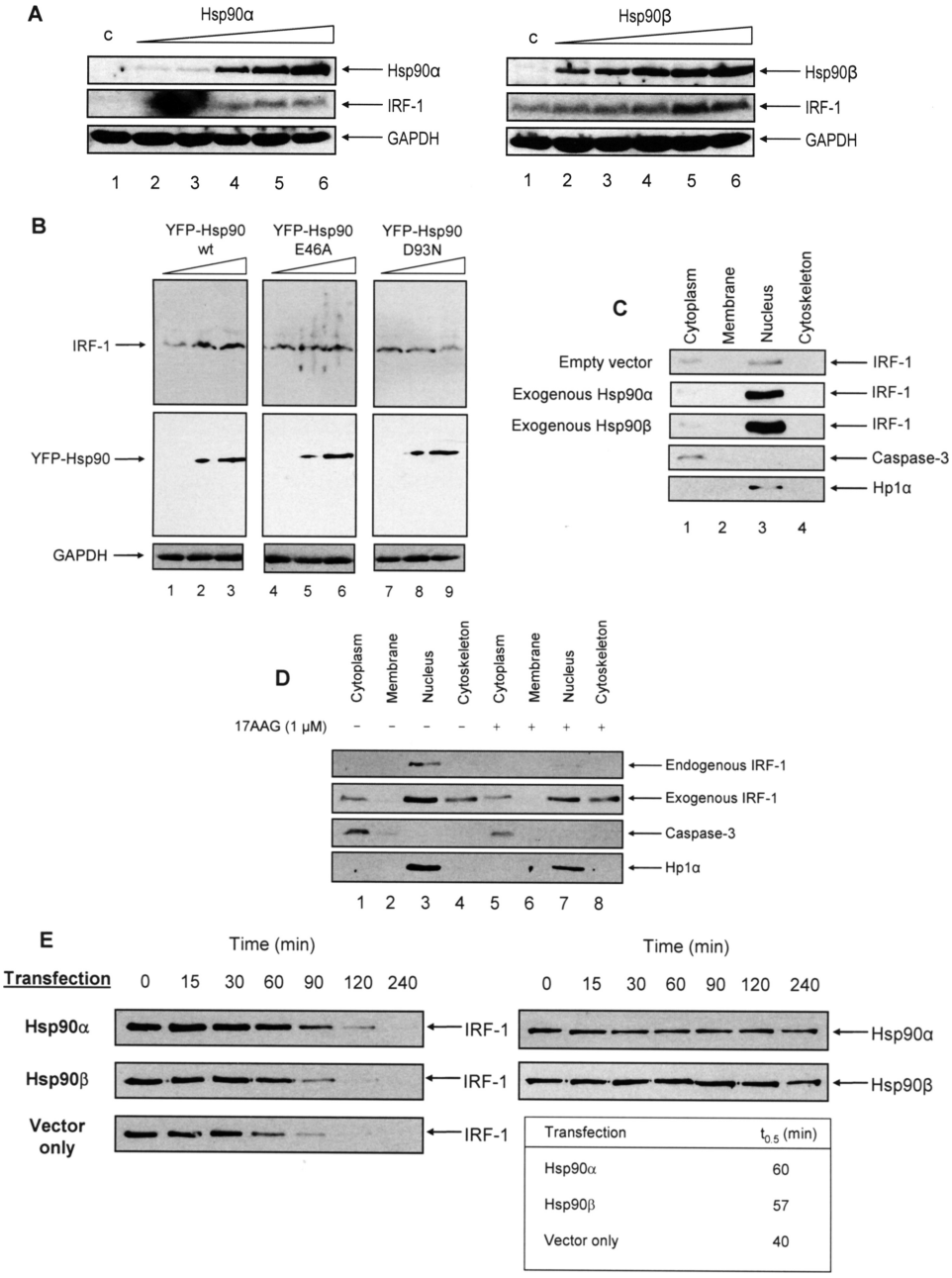

FIGURE 6. **Hsp90 causes IRF-1 nuclear accumulation.** *A,* A375 cells were transiently transfected with a titration (0–10 μg) of FLAG-Hsp90α or -β for 24 h with DNA levels normalized using empty vector. Lysates were analyzed by SDS-PAGE/immunoblot developed using IRF-1 mAb, anti-FLAG, and anti-GAPDH antibodies. The data are representative of at least three separate experiments, and *c* is a mock-transfected control. *B*, A375 cells were transiently transfected with increasing amounts of YFP-Hsp90 (WT or ATP mutants E46A and D93N; 0–5 μg) and analyzed as in *A*. The results are representative of two separate experiments. *C,* A375 cells were transiently transfected with FLAG-Hsp90α or -β or empty vector (5 μg), and 24 h post-transfection the cells were harvested and fractionated using a ProteoExtract kit. The fractions were analyzed by SDS-PAGE/immunoblot developed using IRF-1 mAb, anti-caspase-3, and anti-Hp1α antibodies. *D,* A375 cells were transiently transfected with WT IRF-1 or left untransfected and subsequently treated with 17AAG (1 μM). After 24 h cells were harvested, fractionated, and analyzed as in *C*. Caspase 3 and Hp1α were used as markers for the cytoplasmic and nuclear fractions, respectively. *E,* A375 cells were transiently transfected with a constant amount (5 μg) of FLAG-Hsp90α or -β or empty vector, and 24 h post-transfection, the cells were treated with cycloheximide (30 μg/ml) for the indicated times. Cells were harvested and fractionated as in *C*. The nuclear fraction was analyzed by SDS-PAGE/immunoblot and developed using IRF-1 mAb or anti-FLAG antibody. To calculate the half-life, band intensity was quantified using Scion Imaging software, and ln(% protein remaining) was plotted against time to obtain a linear graph.

DISCUSSION

Despite the fact that IRF-1 is involved in cellular processes ranging from the antiviral response to tumor suppression, only a handful of IRF-1-interacting proteins has been identified. Structure-function analysis has defined the enhancer domain as a key regulatory site involved in controlling IRF-1-dependent effects on gene expression and cell growth. Furthermore, we have defined the Mf1 domain as a distinct region of the enhancer that contains an L*XX*LL motif that is central to both IRF-1-mediated repression of *Cdk2* (15) and the degradation of polyubiquitinated IRF-1 (17). To define components of the IRF-1 interactome whose binding to the Mf1 domain has functional consequences, we set up a biochemical screen for proteins that bind to amino acids 301–320 of IRF-1. Hsp70 was delineated as an L*XX*LL motif-binding protein, and the Mf1 domain was shown to mediate Hsp70/Hsp90-dependent modulation of IRF-1 turnover, activity, and localization.

Studies carried out on the enhancer domain have implicated the Mf1 domain in multifaceted regulation of IRF-1 transcription factor activity and growth suppressor function (15, 17). Thus, deletion of the C-terminal 25 residues impairs the ability of IRF-1 to suppress cell growth in a colony formation assay and also leads to a loss of its *Cdk2* repressor function (12, 15). An L*XX*LL motif embedded within this region appears to be critical for the role of this domain in controlling both IRF-1 biological activity (15) and in determining how IRF-1 is regulated by the ubiquitin proteasome system (17). In this study we have identified proteins that bind to the Mf1 region of IRF-1, prominent among these being members of the molecular chaperone Hsp70 family. Interestingly, although several Hsp70/Hsc70 isoforms are detected in A375 cells (Fig. 2*B*), only one is pulled down efficiently with IRF-1 suggesting that the interaction is specific. In addition, *in vitro* binding assays showed that Hsp70 binding to IRF-1 was an order of magnitude better than Hsc70 binding, although we cannot rule out a role for Hsc70 *in vivo*. Fine mapping of the interaction between Hsp70 and the C terminus of

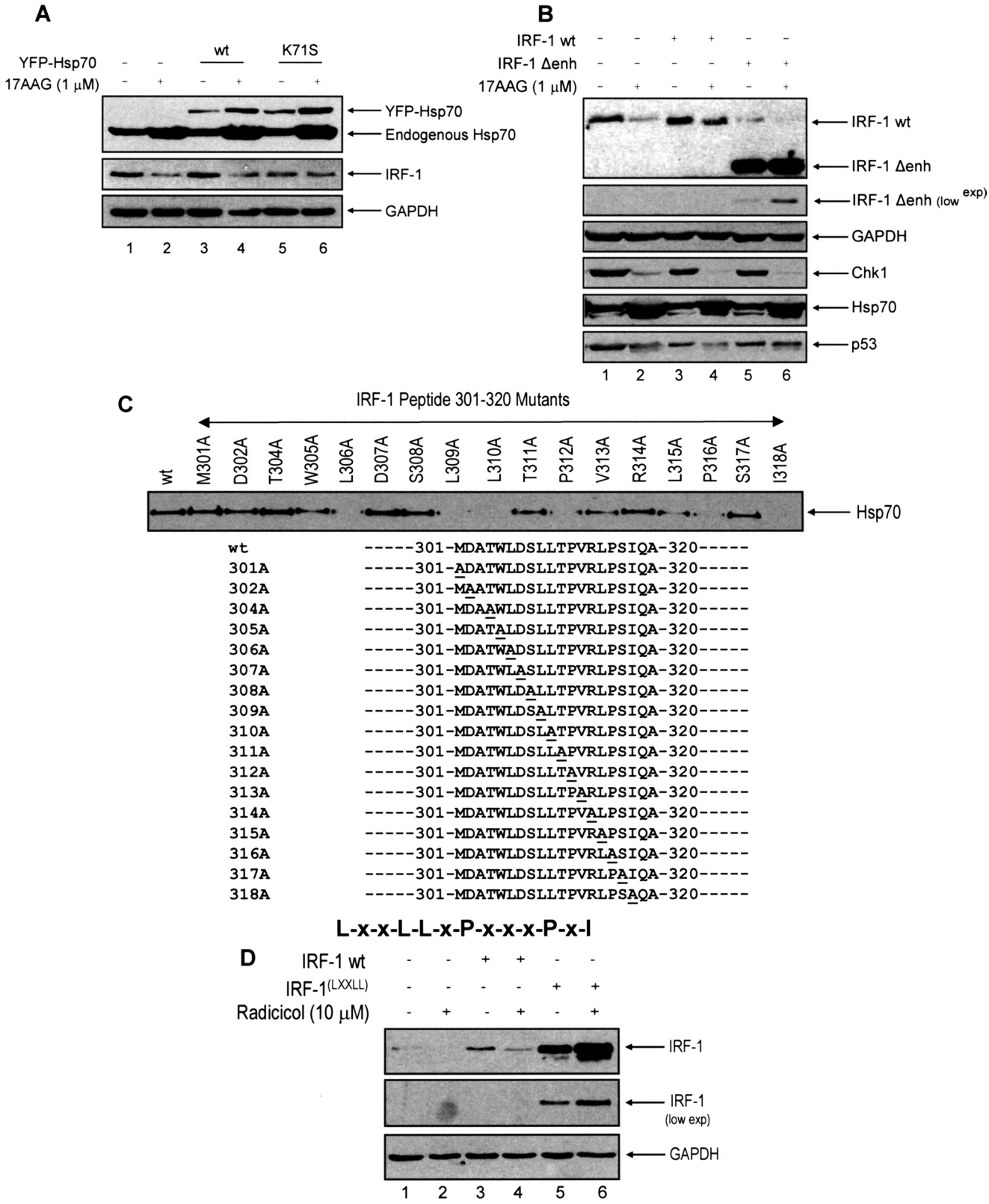

FIGURE 7. **Hsp70-binding motif within the C terminus mediates Hsp70:Hsp90 dependent effects on IRF-1.** *A*, H1299 cells were transiently transfected with YFP-Hsp70 (WT or the dominant negative mutant K71S; 250 ng) or empty vector; 24 h later 17AAG (1 μM) was added and the incubation continued for a further 20 h. Lysates were analyzed by SDS-PAGE/immunoblot developed using IRF-1 mAb, anti-Hsp70, and anti-GAPDH antibodies. *B,* A375 cells were transiently transfected with pcDNA3-IRF-1 WT or Δenh or empty vector and then treated with 17AAG (1 μM) and analyzed as above. The levels of Chk1, Hsp70, and p53 were measured as controls. The data are representative of two separate experiments. *C,* alanine substitutions were introduced into the C-terminal IRF-1 peptide (pep-(301–320)) so that each amino acid was sequentially mutated (*lower panel*) and used to generate a series of affinity columns. Following the isolation of peptide-binding proteins from A375 cell lysate, the columns were eluted, and the eluate was analyzed by SDS-PAGE/immunoblot developed using anti-Hsp70 mAb (SPA-810). A consensus binding site for Hsp70 in IRF-1 is shown. *D,* A375 cells were transiently transfected with IRF-1 WT or an *LXX*LL mutant, and the cells were then treated with radicicol (10 μM) and analyzed as in *B*.

IRF-1 demonstrated that the L*XX*LL motif, along with several proline residues, was an essential component of the interaction. Previous studies have shown that the *E. coli* Hsp70 homologue DnaK binds preferentially to regions with a hydrophobic core of 4–5 amino acids, particularly where these are enriched in leucine residues (34, 35). Interestingly, however, although previous studies using DnaK or recombinant Hsp70 showed a relatively "loose" specificity for Hsp70 binding, in the current study using endogenous Hsp70 from human cells, mutation of specific Leu or Pro residues showed complete loss of Hsp70 binding even though the environment was predominantly hydrophobic. It is interesting to speculate that the difference may reflect post-translational regulation of Hsp70 and its interactions by, for example, cochaperones (21) or post-translational modifications, such as the recently described monoubiquitination of Hsp70 (36).

In this study Hsp90 was able to modulate both IRF-1 turnover and its activity as a transcription factor. In response to 17AAG, in common with other Hsp90 client proteins (37), IRF-1 was targeted for degradation. A requirement for Hsp70 in the 17AAG-activated degradation pathway was demonstrated using a dominant negative Hsp70 construct and by the use of IRF-1 mutant proteins where the C-terminal Hsp70-binding site in the Mf1 domain had been deleted or mutated. Thus degradation of IRF-1 in 17AAG-treated cells most likely involves an Hsp70-associated ubiquitin-protein isopeptide ligase such as CHIP or Parkin (38, 39). Interestingly, prior to the effect of 17AAG on IRF-1 levels, there was a decrease in its transcriptional activity, suggesting that inhibition of Hsp90 has a biphasic effect on IRF-1. At early time points, inhibition of Hsp90 ATPase activity decreases IRF-1 transcriptional activity and is uncoupled from the changes in IRF-1 protein levels that occur at later time points. It will therefore be of interest to determine precisely how blocking the ATPase function of Hsp90 affects IRF-1 conformation and whether this impacts, for example, on the ability of IRF-1 to bind DNA or assemble into a preinitiation complex (see below). The conclusion we have drawn from this is that Hsp90 normally acts as a positive regulator of IRF-1. Supporting this is the observation that overexpression of Hsp90 leads to an increase in the half-life of IRF-1 within the nucleus. Interestingly, the use of dominant negative Hsp70, by itself, was sufficient to reduce the levels of endogenous IRF-1. As the K71S mutant form of Hsp70 is impaired in its ability to fold substrates (40), the data also implicate Hsp70, either by itself or in cooperation with Hsp90, as a positive regulator of IRF-1.

The classic view of the molecular chaperones is that they are primarily involved in the folding of nascent proteins and the prevention of protein aggregation. More recently, the core molecular chaperone machinery, including Hsp70 and Hsp90, has been suggested to take primary responsibility for maintaining a dynamic cellular environment (23, 41) by taking part in transient low affinity protein-protein interactions (25). In addition some members of this group, most notably Hsp90, have more selective roles binding preferentially to specific classes of already folded proteins (42). Large scale screens for novel physical and genetic interactions with Hsp90 in yeast have recently revealed that it interacts with a much greater range of proteins than previously thought. Of particular interest with respect to IRF-1 is the light that these and other studies cast on the role of the chaperones in regulating gene expression (43–45). Together with evidence that Hsp70 can control gene expression through modulation of transcription factor structure and function, these studies also suggest several possible mechanisms by which Hsp70 and/or Hsp90 could affect IRF-1 transactivation. These include the following: control of transcription complex assembly and/or disassembly (24, 46); modulation of sequence-specific DNA binding (27, 47, 48); access to promoter elements within chromosomal DNA (44, 49); or assisting in the post-translational modification of IRF-1 as has been demonstrated for the related transcription factor IRF-3 (50).

Acknowledgments—We thank Prof. Ted Hupp for advice and Dr. Borek Vojtesek for the kind gift of p53 antibodies.

REFERENCES

1. Taniguchi, T., Ogasawara, K., Takaoka, A., and Tanaka, N. (2001) *Annu. Rev. Immunol.* **19,** 623–655
2. Tanaka, N., Ishihara, M., Lamphier, M. S., Nozawa, H., Matsuyama, T., Mak, T. W., Aizawa, S., Tokino, T., Oren, M., and Taniguchi, T. (1996) *Nature* **382,** 816–818
3. Pamment, J., Ramsay, E., Kelleher, M., Dornan, D., and Ball, K. L. (2002) *Oncogene* **21,** 7776–7785
4. Tendler, D. S., Bao, C., Wang, T., Huang, E. L., Ratovitski, E. A., Pardoll, D. A., and Lowenstein, C. J. (2001) *Cancer Res.* **61,** 3682–3688
5. Tanaka, N., Ishihara, M., Kitagawa, M., Harada, H., Kimura, T., Matsuyama, T., Lamphier, M. S., Aizawa, S., Mak, T. W., and Taniguchi, T. (1994) *Cell* **77,** 829–839
6. Passioura, T., Dolnikov, A., Shen, S., and Symonds, G. (2005) *Cancer Res.* **65,** 797–804
7. Nozawa, H., Oda, E., Ueda, S., Tamura, G., Maesawa, C., Muto, T., Taniguchi, T., and Tanaka, N. (1998) *Int. J. Cancer* **77,** 522–527
8. Tamura, G., Sakata, K., Nishizuka, S., Maesawa, C., Suzuki, Y., Terashima, M., Eda, Y., and Satodate, R. (1996) *J. Pathol.* **180,** 371–377
9. Willman, C. L., Sever, C. E., Pallavicini, M. G., Harada, H., Tanaka, N., Slovak, M. L., Yamamoto, H., Harada, K., Meeker, T. C., List, A. F., *et al.* (1993) *Science* **259,** 968–971
10. Fujita, T., Sakakibara, J., Sudo, Y., Miyamoto, M., Kimura, Y., and Taniguchi, T. (1988) *EMBO J.* **7,** 3397–3405
11. Miyamoto, M., Fujita, T., Kimura, Y., Maruyama, M., Harada, H., Sudo, Y., Miyata, T., and Taniguchi, T. (1988) *Cell* **54,** 903–913
12. Xie, R. L., Gupta, S., Miele, A., Shiffman, D., Stein, J. L., Stein, G. S., and van Wijnen, A. J. (2003) *J. Biol. Chem.* **278,** 26589–26596
13. Kirchhoff, S., Oumard, A., Nourbakhsh, M., Levi, B. Z., and Hauser, H. (2000) *Eur. J. Biochem.* **267,** 6753–6761
14. Dornan, D., Eckert, M., Wallace, M., Shimizu, H., Ramsay, E., Hupp, T. R., and Ball, K. L. (2004) *Mol. Cell. Biol.* **24,** 10083–10098
15. Eckert, M., Meek, S. E., and Ball, K. L. (2006) *J. Biol. Chem.* **281,** 23092–23102
16. Nakagawa, K., and Yokosawa, H. (2000) *Eur. J. Biochem.* **267,** 1680–1686
17. Pion, E., Narayan, V., Eckert, M., and Ball, K. L. (2009) *Cell. Signal.* **21,** 1479–1487
18. Wandinger, S. K., Richter, K., and Buchner, J. (2008) *J. Biol. Chem.* **283,** 18473–18477
19. Saibil, H. R. (2008) *Curr. Opin. Struct. Biol.* **18,** 35–42
20. Liberek, K., Lewandowska, A., and Zietkiewicz, S. (2008) *EMBO J.* **27,** 328–335
21. Pratt, W. B., and Toft, D. O. (2003) *Exp. Biol. Med. (Maywood)* **228,** 111–133
22. Vaughan, C. K., Mollapour, M., Smith, J. R., Truman, A., Hu, B., Good, V. M., Panaretou, B., Neckers, L., Clarke, P. A., Workman, P., Piper, P. W., Prodromou, C., and Pearl, L. H. (2008) *Mol. Cell* **31,** 886–895

23. Ellis, R. J. (2006) *Trends Biochem. Sci.* **31,** 395–401
24. Freeman, B. C., and Yamamoto, K. R. (2002) *Science* **296,** 2232–2235
25. Pratt, W. B., Morishima, Y., and Osawa, Y. (2008) *J. Biol. Chem.* **283,** 22885–22889
26. Pearl, L. H., and Prodromou, C. (2006) *Annu. Rev. Biochem.* **75,** 271–294
27. Walerych, D., Kudla, G., Gutkowska, M., Wawrzynow, B., Muller, L., King, F. W., Helwak, A., Boros, J., Zylicz, A., and Zylicz, M. (2004) *J. Biol. Chem.* **279,** 48836–48845
28. Escalante, C. R., Yie, J., Thanos, D., and Aggarwal, A. K. (1998) *Nature* **391,** 103–106
29. Te, J., Jia, L., Rogers, J., Miller, A., and Hartson, S. D. (2007) *J. Proteome Res.* **6,** 1963–1973
30. Neckers, L., Mimnaugh, E., and Schulte, T. W. (1999) *Drug Resist. Updat.* **2,** 165–172
31. Neckers, L., Schulte, T. W., and Mimnaugh, E. (1999) *Invest. New Drugs* **17,** 361–373
32. Heinz, S., Haehnel, V., Karaghiosoff, M., Schwarzfischer, L., Müller, M., Krause, S. W., and Rehli, M. (2003) *J. Biol. Chem.* **278,** 21502–21509
33. Galigniana, M. D., Harrell, J. M., O'Hagen, H. M., Ljungman, M., and Pratt, W. B. (2004) *J. Biol. Chem.* **279,** 22483–22489
34. Rüdiger, S., Germeroth, L., Schneider-Mergener, J., and Bukau, B. (1997) *EMBO J.* **16,** 1501–1507
35. Rüdiger, S., Schneider-Mergener, J., and Bukau, B. (2001) *EMBO J.* **20,** 1042–1050
36. Liu, M., Aneja, R., Sun, X., Xie, S., Wang, H., Wu, X., Dong, J. T., Li, M., Joshi, H. C., and Zhou, J. (2008) *J. Biol. Chem.* **283,** 35783–35788
37. Zhang, H., and Burrows, F. (2004) *J. Mol. Med.* **82,** 488–499
38. Morishima, Y., Wang, A. M., Yu, Z., Pratt, W. B., Osawa, Y., and Lieberman, A. P. (2008) *Hum. Mol. Genet.* **17,** 3942–3952
39. McDonough, H., and Patterson, C. (2003) *Cell Stress Chaperones* **8,** 303–308
40. Klucken, J., Shin, Y., Hyman, B. T., and McLean, P. J. (2004) *Biochem. Biophys. Res. Commun.* **325,** 367–373
41. Dezwaan, D. C., and Freeman, B. C. (2008) *Cell Cycle* **7,** 1006–1012
42. Picard, D. (2006) *Trends Endocrinol. Metab.* **17,** 229–235
43. McClellan, A. J., Xia, Y., Deutschbauer, A. M., Davis, R. W., Gerstein, M., and Frydman, J. (2007) *Cell* **131,** 121–135
44. Zhao, R., Davey, M., Hsu, Y. C., Kaplanek, P., Tong, A., Parsons, A. B., Krogan, N., Cagney, G., Mai, D., Greenblatt, J., Boone, C., Emili, A., and Houry, W. A. (2005) *Cell* **120,** 715–727
45. Zhao, R., and Houry, W. A. (2007) *Adv. Exp. Med. Biol.* **594,** 27–36
46. Stavreva, D. A., Müller, W. G., Hager, G. L., Smith, C. L., and McNally, J. G. (2004) *Mol. Cell. Biol.* **24,** 2682–2697
47. Hansen, S., Hupp, T. R., and Lane, D. P. (1996) *J. Biol. Chem.* **271,** 3917–3924
48. Hupp, T. R., Sparks, A., and Lane, D. P. (1995) *Cell* **83,** 237–245
49. Floer, M., Bryant, G. O., and Ptashne, M. (2008) *Proc. Natl. Acad. Sci. U.S.A.* **105,** 2975–2980
50. Yang, K., Shi, H., Qi, R., Sun, S., Tang, Y., Zhang, B., and Wang, C. (2006) *Mol. Biol. Cell* **17,** 1461–1471